Advances in Aircraft and Spacecraft Science, *Vol. 10, No. 3 (2023) 257-279*
https://doi.org/10.12989/aas.2023.10.3.257

Free vibration analysis of nonlocal viscoelastic nanobeam with holes and elastic foundations by Navier analytical method

Ola A. Siam[1], Rabab A. Shanab[1], Mohamed A. Eltaher*[2,3] and Norhan A. Mohamed[1]

[1]Engineering Mathematics Department, Faculty of Engineering, Zagazig University, Zagazig 44519, Egypt
[2]Mechanical Engineering Department, Faculty of Engineering, King Abdulaziz University,
P.O. Box 80204, Jeddah, Saudi Arabia
[3]Mechanical Design and Production Department, Faculty of Engineering, Zagazig University,
P.O. Box 44519, Zagazig, Egypt

(Received May 14, 2023, Revised June 19, 2023, Accepted June 20, 2023)

Abstract. This manuscript is dedicated to deriving the closed form solutions of free vibration of viscoelastic nanobeam embedded in an elastic medium using nonlocal differential Eringen elasticity theory that not considered before. The kinematic displacements of Euler-Bernoulli and Timoshenko theories are developed to consider the thin nanobeam structure (i.e., zero shear strain/stress) and moderated thick nanobeam (with constant shear strain/stress). To consider the internal damping viscoelastic effect of the structure, Kelvin/Voigt constitutive relation is proposed. The perforation geometry is intended by uniform symmetric squared holes arranged array with equal space. The partial differential equations of motion and boundary conditions of viscoelastic perforated nonlocal nanobeam with elastic foundation are derived by Hamilton principle. Closed form solutions of damped and natural frequencies are evaluated explicitly and verified with prestigious studies. Parametric studies are performed to signify the impact of elastic foundation parameters, viscoelastic coefficients, nanoscale, supporting boundary conditions, and perforation geometry on the dynamic behavior. The closed form solutions can be implemented in the analysis of viscoelastic NEMS/MEMS with perforations and embedded in elastic medium.

Keywords: analytical solutions; dynamic analysis; elastic foundations; Kelvin/Voigt model; perforated nanostructure

1. Introduction

Currently, nanoscience and nanotechnology are promising to explain, understand, and compare the physical and mechanical responses of nanomaterials and nanostructures (MEMS and NEMS) with more precise experimental and theoretical investigation. Hence, to consider and model the size effect of nanostructure accurately, the advanced and modified continuum model theories, such as, nonlocal of elasticity (Eringen 1972, 1983), couple stress theory (Mindlin 1962, Toupin 1962), strain gradient theory (Mindlin 1965, Nix and Gao 1998), and doublet mechanics (Eltaher *et al.* 2020a, b), energy equivalent method (Eltaher *et al.* 2018, Mohamed *et al.* 2019) accounting length

*Corresponding author, Professor, E-mail: mohaeltaher@gmail.com, meltaher@kau.edu.sa

http://www.techno-press.org/?journal=aas&subpage=7 ISSN: 2287-528X (Print), 2287-5271 (Online)

scale should be used, (Daikh *et al.* 2021, Alazwari *et al.* 2022a).

Ebrahimi and Fardshad (2018) studied the thermal effect on buckling and free vibration characteristics of functionally graded (FG) size-dependent Timoshenko nanobeams subjected to an in-plane thermal loading. Ebrahimi *et al.* (2018) examined nonlocal buckling characteristics of heterogeneous plates subjected to various loadings. Ebrahimi and Heidari (2018) investigated the hygro-thermo-mechanical vibration and buckling behavior of embedded FG nanoplates. Alasadi *et al.* (2019) analyzed nonlinear vibrations of metal foam nanobeams with symmetric and non-symmetric porosities. Fenjan *et al.* (2020) studied mechanical-hygro-thermal vibrations of functionally graded porous plates with nonlocal and strain gradient effects. Hosseini *et al.* (2020) investigated axial vibration of a FG nanobeam using nonlocal elasticity theory under clamped-clamped and clamped-free boundary conditions. Nadeem *et al.* (2022) developed an accurate and efficient natural transform homotopy perturbation method for obtaining the numerical solution of nonlinear fractional Newell-Whitehead Segel equation arise in various physical phenomena. Abouelregal *et al.* (2022) developed computational analysis of an infinite magneto-thermoelastic solid periodically dispersed with varying heat flow based on non-local Moore–Gibson–Thompson approach. Hieu *et al.* (2021a) studied the nonlinear vibration of an electrostatically actuated functionally graded (FG) microbeam under longitudinal magnetic field. Hieu *et al.* (2021b) presented the nonlinear bending, vibration and buckling responses of FG nonlocal strain gradient nanobeams resting on an elastic foundation.

The mentioned studies dealt with elastic nanostructures, however, there are some studies for viscoelastic behavior of nanostructures, Khorshidi (2021). To consider the material viscoelastic damping nature and experimental data, the Kelvin-Voigt model is exploited to develop the Young's modulus, Abouelregal and Sedighi (2022). Assie *et al.* (2010a, b) studied numerically by FEM the response of viscoelastic structures under impact by using generalized standard linear solid model. Ansari *et al.* (2015, 2016) developed semi-analytical technique to predict the natural frequencies of viscoelastic Euler and Timoshenko nonlocal nanobeam. Zenkour (2017) examined vibration response of generalized thermoelastic microbeams resting on visco-Pasternak. Malikan *et al.* (2018) investigated the thermos-dynamic response of nonlocal strain gradient SWCNTs rested on viscoelastic foundation. Malikan and Far (2018) examined the dynamic buckling of nonlocal graphene sheet rested on viscoelastic medium using differential quadrature method. Ebrahimi *et al.* (2021) studied the damping forced harmonic response of magneto-electro-viscoelastic on nonlocal strain gradient nanobeam embedded on viscoelastic Winkler–Pasternak foundation. Bagheri and Beni (2021) presented the nanoscale size-dependency on the nonlinear forced response of viscoelastic flexoelectric modified couple nanobeams by using Euler–Bernoulli theory and Galerkin's method. Behdad *et al.* (2021) used a two-phase local/nonlocal elasticity to capture the size-dependent dynamic stability and damping of viscoelastic functionally graded (FG) Timoshenko nanobeams using Kelvin-Voigt model. Reza *et al.* (2021) presented the effect of viscoelastic behavior of polymer matrix of unidirectional fiber-reinforced laminated composite on stress distribution around the pin-loaded hole under tensile loading.

Noroozi and Ghadiri (2021) studied forced vibration response of an axial moving viscoelastic nonlocal nanobeam using Galerkin's method. Abouelregal and Sedighi (2022) exploited Kelvin-Voigt viscoelastic model in analyzing thermoelastic characteristics of moving viscoelastic nonlocal couple stress nanobeams using the Laplace transform. Jalaei *et al.* (2022) examined the transient response of viscoelastic FG nonlocal strain gradient nanobeams subjected to dynamic loads and magnetic. Ali *et al.* (2022) studied the effects of viscoelastic bonding layer on performance of piezoelectric actuator attached to elastic structure using a finite element procedure. Martin (2022) exploited nonlocal fractional Zener model to study nonlinear vibrations of viscoelastic Euler–Bernoulli nanotube resting on a Kelvin–Voigt foundation. Rahmani *et al.* (2022) presented the size effect on wave propagation of a magneto-electro-thermo-elastic nanobeam embedded in viscoelastic medium using modified couple stress and nonlocal theories. Wu *et al.* (2022) applied the Kelvin–Voigt model and nonlocal strain gradient theory to investigate size-dependent vibration response of viscoelastic nanobeam. Eltaher *et al.* (2022) developed analytical solutions for the free vibration of viscoelastic perforated thin/thick nanobeam structures. You *et al.* (2022) presented a novel time-domain homogenization model combining the viscoelastic constitutive law with Eshelby's inclusion theory-based micromechanics model to predict the mechanical behavior of the particle reinforced composite material.

Structures embedded on the elastic foundations are extensively used in the engineering field and research. Researchers use different models to simulate elastic foundations, Hossain and Lellep (2021). Alzahrani *et al.* (2013) investigated the effect of size-scale on bending of embedded in two-parameter elastic medium and under hygro-thermo-mechanical loads. Mohammadi *et al.* (2014) explored the postbuckling instability of nonlinear Euler–Bernoulli nonlocal nanobeam embedded in elastic foundation. Mechab *et al.* (2016) developed probabilistic analysis to study free vibration of FGM nanoplate resting on Winkler–Pasternak elastic foundations. Togun (2016), Togun and Bağdatlı (2016) examined free and forced vibration of nonlocal Euler-Bernoulli nanobeam resting on an elastic foundation of the Pasternak type by using a perturbation technique. Demir *et al.* (2018) developed the finite element model to study the static bending of nonlocal nanobeams under the Winkler foundation and the uniform load. Mohamed *et al.* (2018) studied the nonlinear vibration responses of buckled Euler–Bernoulli beams resting on nonlinear elastic foundations using the differential-integral quadrature method (DIQM) and Newton's method. Abdelrahman *et al.* (2020) studied analytically the influence of moving load on dynamics of Timoshenko CNTs embedded in elastic media based on doublet mechanics theory. Khadir *et al.* (2021), Alazwari *et al.* (2022) studied the mechanical responses of quasi 3D higher-order shear deformation of FG-CNTs reinforced composite nanoplates rested on two-dimensional variable Winkler elastic foundation. Ramezannejad and Heidari (2022) studied the nonlinear primary frequency response analysis of self- sustaining nanobeam rested on viscoelastic foundation and considering surface elasticity. Darban *et al.* (2022) studied the buckling of Bernoulli-Euler nonlocal stress-driven gradient nanobeam resting on the Pasternak elastic foundation. Assie *et al.* (2023) investigated the static stability of bi-directional functionally graded porous plate resting on elastic foundation by using unified shear deformation theories. Zheng *et al.* (2023) explained the size-dependent nonlinear bending of magneto-electro-elastic laminated nanobeams rested on elastic. Abouelregal *et al.* (2023) examined examine the micromechanical coupling and the influence of thermo-mechanical relaxation, a higher-order two-phase-lag thermoelastic concept and a viscoelastic model of Kelvin–Voigt type. Ding *et al.* (2023) examined effect of spinning motion and initial geometric imperfections on nonlinear low-velocity impact of graphene platelets reinforced metal foams cylindrical shell.

From the literature, it is revealed that the dynamic response of viscoelastic perforated nonlocal nanobeams resting on elastic foundations has not been studied elsewhere. Therefore, the present article aims to cover this point clearly. In the next sections, the problem formulations including the geometrical adaptation, kinematic relations, and nonlocal constitutive equation will be presented in section 2. The derived equations of motion and solution methodology will be discussed in sections 3 and 4. The validation and parametric analysis to show the influence of elastic foundations parameters, nonlocal scale, perforation parameters on the natural frequencies of nanobeams with

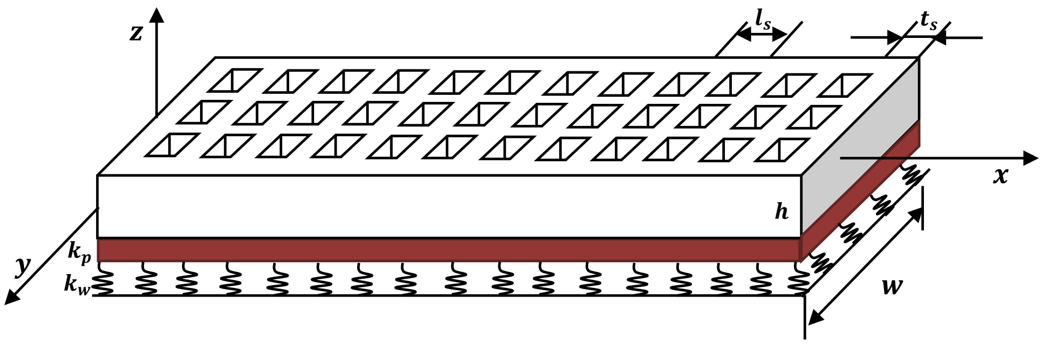

Fig. 1 A perforated beam with the geometrical parameters (Eltaher and Mohamed 2020)

different boundary conditions will be illustrated and discussed in section 5.

2. Problem formulation

2.1 Geometrical adaptation

A perforated nanobeam geometry is illustrated in Fig. 1. As seen, nanobeam has a length of L, width of *w* and thickness of h. A nanobeam is holed with square holes in regular pattern, that has spatial period l_s and side $l_s - t_s$, and a number of hole-rows *N* along the section. The filling ratio which is defined as the ratio of material thickness between two holes to the period length, can be formulated as, Almitani *et al.* (2019, 2020)

$$\alpha = \frac{t_s}{l_s} \quad 0 \leq \alpha \leq 1 \tag{1}$$

that means the beam is completely filled at filling ratio $\alpha = 1$, partially filling when $0 \leq \alpha \leq 1$, and completely perforated at $\alpha = 0$. Under the hypothesis of total stress along the cross section is the same for both complete beam and perforated one and a linear continuous stress distribution, the relative equivalent bending stiffnesscan be depicted by (Abdalrahmaan *et al.* 2020, 2021) as

$$(EI)_r = (EI)_{eq}/EI = \frac{\alpha(N+1)(N^2+2N+\alpha^2)}{(1-\alpha^2+\alpha^3)N^3+3\alpha N^2+(3+2\alpha-3\alpha^2+\alpha^3)\alpha^2 N+\alpha^3} \tag{2}$$

Considering the relative shear effect of perforated nanobeam,the shear stiffness will be modified as (Esen *et al.* 2020)

$$(GA)_r = (GA)_{eq}/GA = \frac{\alpha^3(N+1)}{2N} \tag{3}$$

It is noted that from Eq. (3), the shear stiffness is dependent on both filling ratio and number of holes. But the filling ratio is more pronounced on the shear stiffness than the number of holes. The relative mass of the perforated beam per unit length to the standard beam can be modified as (Eltaher 2020a, b)

$$(\rho A)_r = (\rho A)_{eq}/\rho A = \frac{[1-N(\alpha-2)]\alpha}{N+\alpha} \tag{4}$$

The relative equivalent moment of inertia per unit length can be calculated by integrating over a strip of N square cells of length l_s, (Abdalrahmaan *et al.* 2019)

$$(\rho I)_r = (\rho I)_{eq}/\rho I = \frac{\alpha\left[(2-\alpha)N^3+3N^2-2(\alpha-3)\left(\alpha^2-\alpha+1\right)N+\alpha^2+1\right]}{(N+\alpha)^3} \tag{5}$$

2.2 Kinematic assumptions for thin/thick beam

In case of thin beam, kinematics assumptions of Euler-Bernoulli theory can be applied as follows

$$u(x,z,t) = u_0(x,t) - z\frac{\partial w_0(x,t)}{\partial x} \tag{6a}$$

$$w(x,z,t) = w_0(x,t) \tag{6b}$$

In which u is the inplane and$w$ is the out of plane displacements at any generic point. u_0 and w_0 are displacements along the neutral axis. Since the axial displacement along neutral axis is very small comparable with transverse displacement and rotation, so it can be neglected. The strain can be defined by

$$\varepsilon_{xx} = \frac{\partial u(x,z,t)}{\partial x} = \frac{\partial u_0(x,t)}{\partial x} - z\frac{\partial^2 w_0(x,t)}{\partial x^2} = \varepsilon_{xx}^0 + zk_0 \tag{7}$$

As the thickness to length of the beam reduces to less than 20, the shear effect should be considered, and kinematics assumptions of Timoshenko beam theory can be applied as following

$$u(x,z,t) = u_0(x,t) + z\phi(x,t) \tag{8a}$$

$$w(x,z,t) = w_0(x,t) \tag{8b}$$

in which ϕ is the rotation of the cross section. Based on Eq. (8), the nonzero strains are

$$\varepsilon_{xx} = \frac{\partial u(x,z,t)}{\partial x} = \frac{\partial u_0(x,t)}{\partial x} + z\frac{\partial \phi(x,t)}{\partial x} \tag{9a}$$

$$\varepsilon_{xz} = \frac{1}{2}\left[\frac{\partial u(x,z,t)}{\partial z} + \frac{\partial w(x,z,t)}{\partial x}\right] = \frac{1}{2}\left[\phi(x,t) + \frac{\partial w_0(x,t)}{\partial x}\right] = \frac{1}{2}\gamma_{xz} \tag{9b}$$

According to Eq. (9b), the shear is constant through the beam thickness, which is impractical. To compensate the error due to constant shear, the shear correction factor is proposed.

2.3 Nonlocal constitutive equations

The basis of nonlocal elasticity assumed that the stress at a point is a functional of strain field at every point in body domain. The nonlocal constitutive equation can be depicted by (Danesh and Javanbakht 2021)

$$\sigma_{ij}(x) = \int_V \alpha(|x'-x|,\tau)t_{ij}(x')\mathrm{d}x' \tag{10}$$

in which $t_{ij}(x')$ are the macroscopic stress tensor at point x and $\alpha(|x'-x|,\tau)$ is nonlocal modulus function that represents the effect of interatomic bonding. τ is a material length scale constant. The macroscopic stress tensor can be described as a function of material elasticity tensor (C) and strain (ε) by generalized Hooke's law as

$$t(x) = C(x):\varepsilon(x) \tag{11}$$

In (1983) Eringen proved that when nonlocal modulus described by a Green's function, the nonlocal constitutive relation can be reduced to the differential form as

$$[1-(e_0 a)^2\,\nabla^2]\sigma_{ij}=t_{ij} \tag{12}$$

Where e_0 is constant to match the reliable results by experiments, a is the internallength scale, and ∇^2 is the Laplacian operator. For one-dimensional nonlocal nanobeam, nonlocal constitute relation (Eq. (12)) can be written as (Abdelrahman *et al.* 2021),

$$\sigma_{xx}-\mu\frac{\partial^2\sigma_{xx}}{\partial x^2}=E\varepsilon_{xx},\quad [\mu=(e_0 a)^2] \tag{13a}$$

$$\sigma_{xz}-\mu\frac{\partial^2\sigma_{xz}}{\partial x^2}=G\gamma_{xz} \tag{13b}$$

3. Governing equations

The governing equation of motion of viscoelastic perforated thin nanobeam can be presented by the following

$$(EA)_{eq}\frac{\partial^2 u_o}{\partial x^2}+\left(1-\mu\frac{\partial^2}{\partial x^2}\right)f=\left(1-\mu\frac{\partial^2}{\partial x^2}\right)I_0\frac{\partial^2 u_o}{\partial t^2} \tag{14a}$$

$$-(EI)_{eq}\frac{\partial^4 w_o}{\partial x^4}+\left(1-\mu\frac{\partial^2}{\partial x^2}\right)\left[P-N_b\frac{\partial^2 w_o}{\partial x^2}-K_W w_0+K_P\frac{\partial^2 w_0}{\partial x^2}\right]=\left(1-\mu\frac{\partial^2}{\partial x^2}\right)\left[I_0\frac{\partial^2 w_o}{\partial t^2}-I_2\frac{\partial^4 w_o}{\partial x^2\partial t^2}\right] \tag{14b}$$

where the governing equation of motion of viscoelastic perforated thick nanobeam can be derived as

$$(EA)_{eq}\frac{\partial^2 u_o}{\partial x^2}+\left[1-\mu\frac{\partial^2}{\partial x^2}\right]f=\left[1-\mu\frac{\partial^2}{\partial x^2}\right]I_0\frac{\partial^2 u_o}{\partial t^2} \tag{15a}$$

$$(GA)_{eq}k_s\left(\frac{\partial\phi}{\partial x}+\frac{\partial^2 w_0}{\partial x^2}\right)+\left(1-\mu\frac{\partial^2}{\partial x^2}\right)\left[P(x,t)-N_b\frac{\partial^2 w_0}{\partial x^2}-K_W w_0+K_P\frac{\partial^2 w_0}{\partial x^2}\right]=\left(1-\mu\frac{\partial^2}{\partial x^2}\right)I_0\frac{\partial^2 w_0}{\partial t^2} \tag{15b}$$

$$(EI)_{eq}\frac{\partial^2\phi}{\partial x^2}-(GA)_{eq}k_s\left(1+g\frac{\partial}{\partial t}\right)\left(\phi+\frac{\partial w_0}{\partial x}\right)=\left(1-\mu\frac{\partial^2}{\partial x^2}\right)I_2\frac{\partial^2\phi}{\partial t^2} \tag{15c}$$

The following mathematical more is limited to analyzing the linear static and free vibration responses of thin and moderated thick nanobeam with viscoelastic materials and rested on elastic foundation. The model considers the microstructure and length scale parameters. However, the nonlinear analysis, multi-physics loads, and post-buckling responses can't be predicted by the following model.

4. Solution methodology

4.1 Exact solutions for free vibration of viscoelastic PEBNB

Based on The Navier's method, a general exact solution of PEBNB beam for different types of

Table 1 The shape function $\theta_n(x)$ for different boundary conditions, Abo-bakr *et al.* (2021)

BC	Shape function, $\theta_n(x)$
SS	$\sin(\alpha_n x), \alpha_n = n\pi/L$
CC	$\cosh(\alpha_n x) - \cos(\alpha_n x) - \xi_n[\sinh(\alpha_n x) - \sin(\alpha_n x)], \xi_n = \frac{\sin(\alpha_n L) - \sinh(\alpha_n L)}{\cos(\alpha_n L) - \cosh(\alpha_n L)},$ $\alpha_n = (n + 0.5)\pi/L$
CS	$\cosh(\alpha_n x) - \cos(\alpha_n x) - \xi_n[\sinh(\alpha_n x) - \sin(\alpha_n x)], \xi_n = \frac{\sin(\alpha_n L) + \sinh(\alpha_n L)}{\cos(\alpha_n L) + \cosh(\alpha_n L)},$ $\alpha_n = (n + 0.25)\pi/L$

boundary conditions is obtained. The obtained closed form frequency expression is valid for simply supported (SS), clamped-clamped (CC) and clamped-simply (CS) boundary conditions. Due to the decoupling between Eq. (15a) and Eq. (15b) and to get the closed form solution, the suggested series for displacement function $w_0(x,t)$ that satisfy the boundary conditions at $x = 0, L$ can be defined by, Shanab and Attia (2020)

$$w_0(x,t) = \sum_{n=1}^{\infty} W_n \theta_n(x) e^{i\lambda_n t} \tag{17}$$

where λ_n is the natural frequency of the beam, $i = \sqrt{-1}$, W_n is the unknown Fourier coefficients to be determined and the function $\theta_n(x)$ for different boundary conditions is defined as in Table 1.

By substituting $\theta_n(x)$, from Table 1, into Eq. (15b), setting all external forces to zero, then multiplying the resulting equation by $\theta_m(x)$ and integrating with respect to x from 0 to L, one obtains the exact form of fundamental frequency of PTNNB as follows

$$\lambda_n = \sqrt{\frac{\int_0^L [(EI)_{eq}\theta_n'''' - K_P(\theta_n'' - \mu\theta_n'''') + K_W(\theta_n - \mu\theta_n'')]\theta_m dx}{\int_0^L [-I_2\theta_n'' - \mu(I_0\theta_n'' - I_2\theta_n'''' + I_0\theta_n)]\theta_m dx}} \tag{18}$$

4.2 Exact solutions for free vibration of viscoelastic PTKNB

The system of governing equations, Eq. (16) is solved analytically using Navier's method for different types of boundary conditions. The displacement functions are approximated as a series in the following form

$$\begin{cases} w_0(x,t) = \sum_{n=1}^{\infty} W_n \theta_n(x) e^{i\lambda_n t} \\ \phi(x,t) = \sum_{n=1}^{\infty} \Phi_n \frac{\partial \theta_n(x)}{\partial x} e^{i\lambda_n t} \end{cases} \tag{19}$$

where λ_n is the natural frequency of the beam, $i = \sqrt{-1}$, and $\{W_n, \Phi_n\}$ are the unknown Fourier coefficients to be determined. The shape functions $\theta_n(x)$ for different boundary conditions is pre-defined in Table 1.

To obtain the fundamental frequencies of PTKNB, Eq. (19) in conjunction with the expression of $\theta_n(x)$, Table 1, are substituted into Eqs. (16b), (16c) for different boundary conditions. Then multiplying the resulting equations by $\theta_m(x)$, $\frac{\partial \theta_m(x)}{\partial x}$, respectively. Finally, integrating these equations with respect to x from 0 to L. The following system of linear system of algebraic equations is obtained

$$\begin{bmatrix} k_{11} + m_1 {\lambda_n}^2 & k_{12} \\ k_{21} & k_{22} + m_2 {\lambda_n}^2 \end{bmatrix} \begin{Bmatrix} W_n \\ \Phi_n \end{Bmatrix} = \mathbf{0} \tag{20}$$

in which

$$\begin{Bmatrix} k_{11} \\ k_{12} \\ k_{21} \\ k_{22} \end{Bmatrix} = \int_0^L \begin{Bmatrix} \left[(GA)_{eq} k_s \theta_n'' + K_P(\theta_n'' - \mu\theta_n'''') - K_W(\theta_n(x) - \mu\theta_n'')\right]\theta_m \\ (GA)_{eq} k_s \theta_n'' \theta_m \\ -(GA)_{eq} k_s \theta_n' \theta_m' \\ \left((EI)_{eq}\theta_n''' - (GA)_{eq} k_s \theta_n'\right)\theta_m' \end{Bmatrix} dx \tag{21a}$$

$$\begin{Bmatrix} m_1 \\ m_2 \end{Bmatrix} = \int_0^L \begin{Bmatrix} I_0(\theta_n - \mu\theta_n'')\theta_m \\ I_2(\theta_n' - \mu\theta_n''')\theta_m' \end{Bmatrix} dx \tag{21b}$$

To obtain a non-trivial solution, the determinant of the coefficient matrix of Eq. (20), must be zero. Then, the exact form of the fundamental frequencies for different types of boundary conditions is obtained as

$$\lambda_n = \sqrt{\frac{-(k_{11}m_2 + k_{22}m_1) - \sqrt{(k_{11}m_2 + k_{22}m_1)^2 - 4m_1m_2(k_{11}k_{22} - k_{12}k_{21})}}{2m_1m_2}} \tag{22}$$

5. Numerical results and validation

This section validated the proposed model with the pervious works for elastic solid nanobeam for a thin and a thick structure. Also, parametric studies are performed to show the effects of elastic foundation parameters, number of holes, filling ratio, length scale parameter, and beam theories on the natural frequencies of nanobeams for the different boundary conditions.

5.1 Modal validation

Tables 2 and 3 listed the frequency expression of a nonlocal Euler-Bernoulli/Timoshenko solid beams structure with different boundary conditions at different nonlocal parameter values. As shown in Table 2, the present results are in good agreement with Shanab *et al.* (2020b) and Mohamed *et al.* (2016) for Euler-Bernoulli beams. Also, Table 3 shows that the frequency reduced by increasing the nonlocal parameter for both thin and thick beams. It is noticed in Table 3 that, at the same nonlocal parameter, the frequency of Euler beam is higher than that of Timoshenko beam, due to shear effect.

The validation of the fundamental linear frequency for Timoshenko beam surrounded by elastic foundation is presented in Table 4 and accuracy results are achieved with the validated literatures. According to the present results which are listed for different boundary conditions, the current analytical procedure can be used to analyze natural frequencies of perforated viscoelastic nanobeams.

5.2 Parametric studies

Throughout the parametric study $E = 30$ Mga, $h = 1,\ \rho = 1,\ L = 20h,\ \nu = 0.3,\ K_W =$

Table 2 Comparison of the dimensionless fundamental frequencies $\omega = \lambda L^2\sqrt{\rho A_0/EI}$ of solid uniform beams ($L = 10, L/h = 20, b = h, E = 30$ MPa, $\rho = 1, \nu = 0.3$)

	Simply supported			Clamped-clamped		
	Mode1	Mode2	Mode3	Mode1	Mode2	Mode3
	Nonlocal parameter $\mu = 0$					
Present PTNNB	9.8595	39.3171	88.0158	22.1757	61.3948	119.6907
Present PTKNB	9.8281	38.8299	85.6619	21.8413	59.5811	113.8628
Shanab *et al.* (2020b)	9.8595	39.3171	88.0158	22.3447	61.3790	119.6766
Mohamed *et al.* (2016)	9.8595	39.3171	88.0158	22.3447	61.3790	119.6760
Eltaher (2013b)	9.8798	39.6460	89.7046	22.4022	61.9872	122.2778
Reddy (2011)	9.8600	39.3200	88.0200	-	-	-
	Nonlocal parameter $\mu = 2$					
Present PTNNB	9.0102	29.3905	52.8213	19.6872	44.3448	69.3973
Present PTKNB	8.9816	29.0263	51.4087	19.5696	42.9162	65.7994
Mohamed *et al.* (2016)	9.0102	29.3905	52.8208	19.9954	44.1031	69.1806
Eltaher (2013b)	9.0257	29.5252	53.1629	20.0368	44.3229	69.6261

Table 3 Comparison of the dimensionless fundamental circular frequencies $\sqrt{\omega}_1 = L\sqrt{\lambda_1\sqrt{\rho A_0/EI}}$ of solid uniform Euler beam ($L = 10\ m$, E=30 MPa, $\rho = 1, h = 0.1, \nu = 0.3$)

BC		Nonlocal parameter					
		$\mu = 0$	$\mu = 1$	$\mu = 2$	$\mu = 3$	$\mu = 4$	$\mu = 5$
SS	Present PTNNB	3.1415	3.0685	3.0032	2.9443	2.8908	2.8418
	Present PTKNB	3.1413	3.0683	3.0030	2.9441	2.8906	2.8416
	Behera and Chakraverty (2015)	3.1416	3.0685	3.0032	2.9444	2.8908	2.8418
CC	Present PTNNB	4.7123	4.5784	4.4616	4.3584	4.2661	4.1828
	Present PTKNB	4.7052	4.5715	4.4549	4.3518	4.2596	4.1765
	Behera and Chakraverty (2015)	4.7300	4.5945	4.4758	4.3707	4.2766	4.1917
CS	Present PTNNB	3.9269	3.8231	3.7317	3.6503	3.5770	3.5106
	Present PTKNB	3.9295	3.9295	3.7342	3.6527	3.5794	3.5129
	Behera and Chakraverty (2015)	3.9266	3.8209	3.7278	3.6448	3.5701	3.5024

Table 4 Comparison of fundamental linear frequency $\sqrt{\omega}_1 = L\sqrt{\lambda_1\sqrt{\rho A_0/EI}}$ for Timoshenko beam surrounded by elastic foundations, (E = 90 GPa, ρ =2700 kg/m^3, ν=0.23, L=120h, $b = 2h, k_s = \frac{5}{6}$, μ =0, $K_W = \frac{k_w(EI)}{L^4}, K_P = \pi^2\frac{k_p(EI)}{L^2}$)

k_p	$k_w = 0$				$k_w = 10^2$				$k_w = 10^4$			
	Shanab *et al.*	Chen *et al.* (2004)	Present PTNNB	Present PTKNB	Shanab *et al.*	Chen *et al.* (2004)	Present PTNNB	Present PTKNB	Shanab *et al.*	Chen *et al.* (2004)	Present PTNNB	Present PTKNB
0	3.1414	3.1414	3.1415	3.1414	3.7482	3.7482	3.7483	3.7482	10.0241	10.0240	10.0241	10.0241
0.5	3.4766	3.4766	3.4767	3.4766	3.9607	3.9607	3.9608	3.9607	10.0362	10.0361	10.0362	10.0362
1.0	3.7359	3.7359	3.7360	3.7359	4.1436	4.1436	4.1436	4.1436	10.0482	10.0481	10.0482	10.0482
2.5	4.2969	4.2969	4.2970	4.2969	4.5823	4.5823	4.5823	4.5823	10.0840	10.0839	10.0840	10.0840

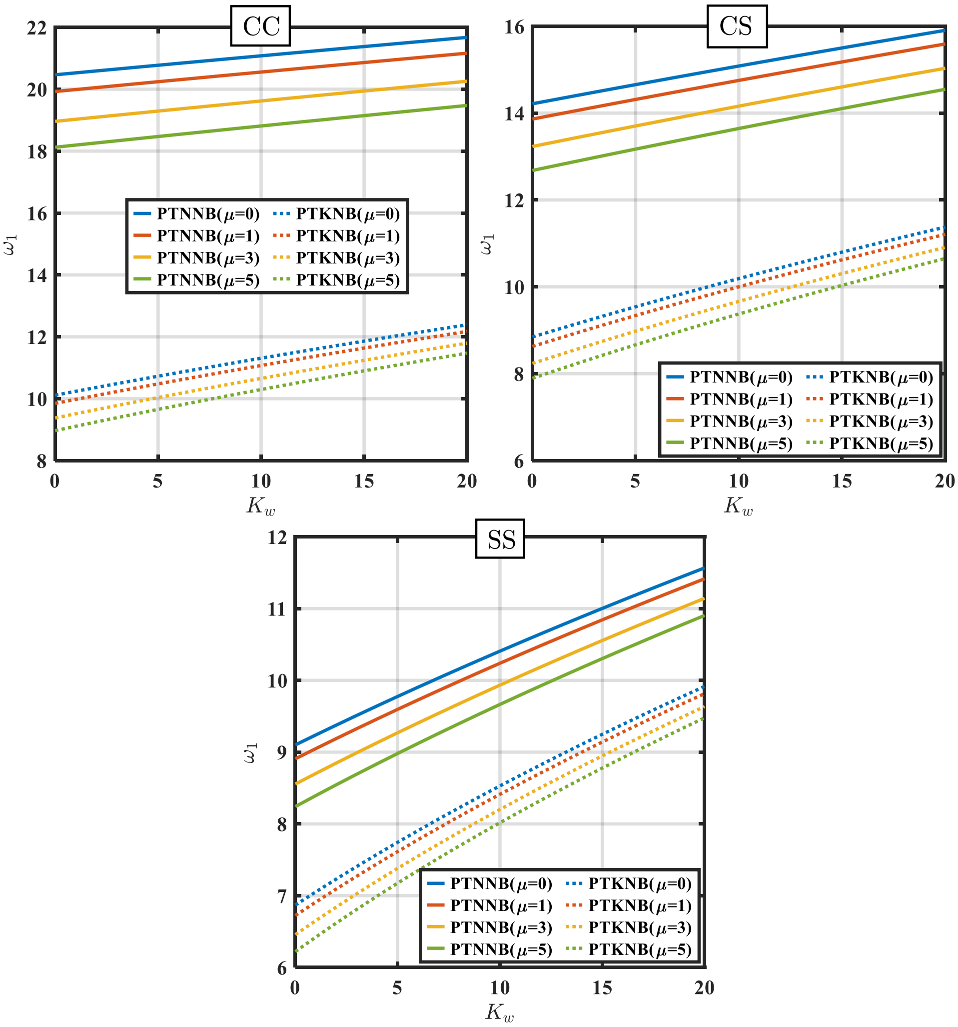

Fig. 2 Variation of the natural frequency parameter of the 1st mode with Winkler foundation parameter k_w for both PTNNB and PTKNB for CC, CS and SS boundary conditions at $N_0 = 4$, α=0.2, μ=0,1, 3, 5 and L/h=15

$\frac{k_w(EI)}{L^4}, K_P = \frac{k_p(EI)}{L^2}, \ \omega = \lambda L^2\sqrt{\rho A_0/EI}.$

5.2.1 Effect of Winkler foundation (Kp=0) on PTNNB and PTKNB

Figs. 2, 3, 4 illustrate the effect of Winkler foundation on the natural frequency of perforated thin and thick nanobeams at 1st, 2nd, and 3rd mode, respectively and different nonlocal parameters. As shown in Fig. 2, by increasing Winkler foundation, the natural frequency increased significantly in semi- linear behavior for PTNNB and PTKNB. However, the Winkler foundation has insignificant effect in 2nd and 3rd mode frequencies for PTNNB and PTKNB. In addition, it is obvious from Figs. 2-3 that the influence of the nonlocal parameter on the frequency of PTNNB is higher than those of PTKNB.

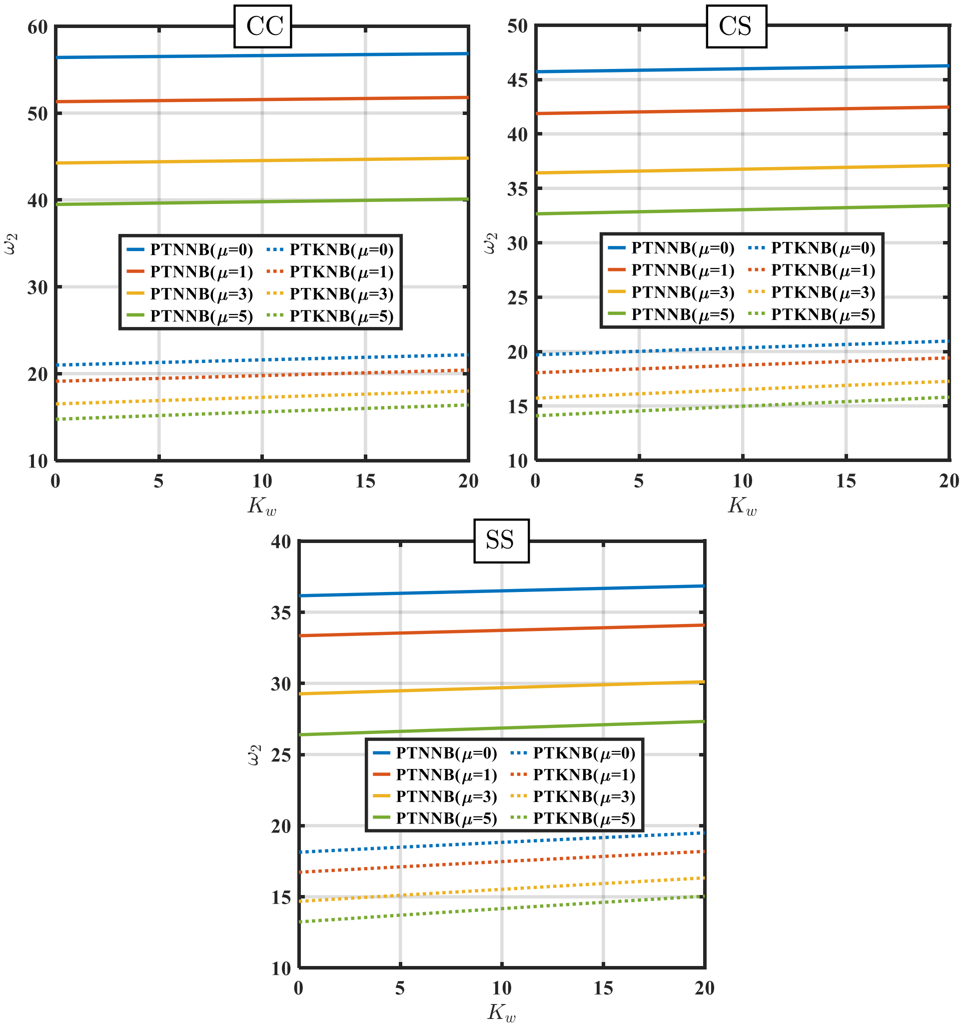

Fig. 3 Variation of the natural frequency parameter of the 2nd mode with Winkler foundation parameter k_w for both PTNNB and PTKNB for CC, CS and SS boundary conditions at $N_0 = 4$, α=0.2, μ=0,1, 2, 3 and *L/h*=15

5.2.2 Effect of Pasternak foundation (Kw=0) on PTNNB and PTKNB

The effect of the Pasternak foundation on the first three fundamental frequemcies at different nonlocal parameter are presented in Figs. 5-7 for perforated thin and thick nanobeams. As shown, by increasing the Pasternak foundation, the natural frequency is increased significantly in semi-linear behavior for PTNNB and PTKNB. Also, by increasing the nonlocal parameter the frequency increases for PTNNB and PTKNB.

5.2.3 Effect of filling ratio on PTNNB and PTKNB

Figs. 8-10 illustrate the effect of the filling ratio on the first three natural frequencies of perforated thin and thick nanobeams at different beam aspect ratios. As shown, for CC, CS boundary condition by increasing the filling ratio, the natural frequency decreases in the case of

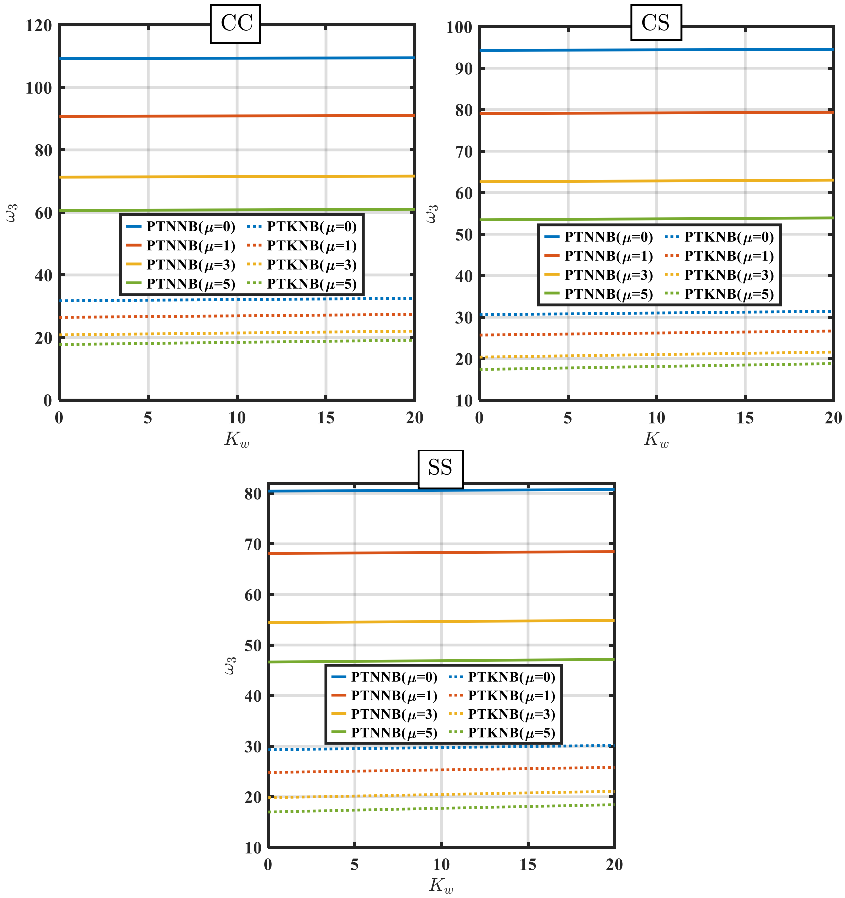

Fig. 4 Variation of the natural frequency parameter of the 3rd mode with Winkler foundation parameter k_w for both PTNNB and PTKNB for CC, CS and SS boundary conditions at $N_0 = 4$, α=0.2, μ=0,1, 2, 3 and *L*/*h*=15

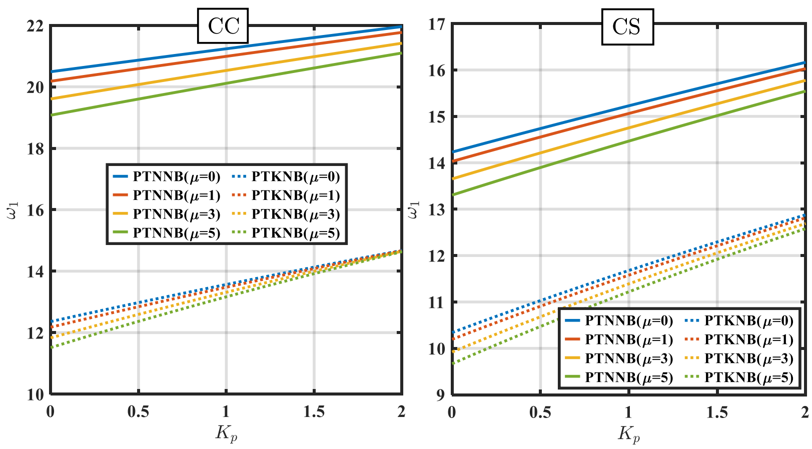

Fig. 5 Variation of the natural frequency parameter of the 1st mode with Pasternak foundation parameter k_p for both PTNNB and PTKNB for CC, CS and SS boundary conditions at $N_0 = 4$, α=0.2, μ=0,1, 3,5 and *L*/*h*=15

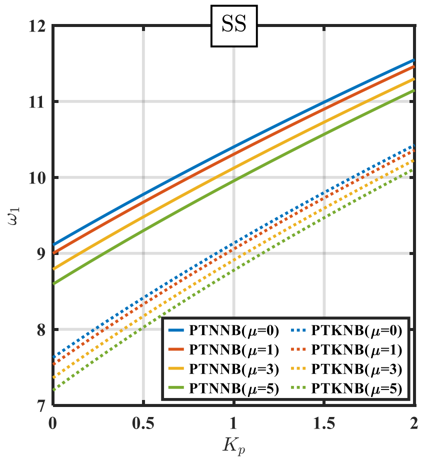

Fig. 5 Continued

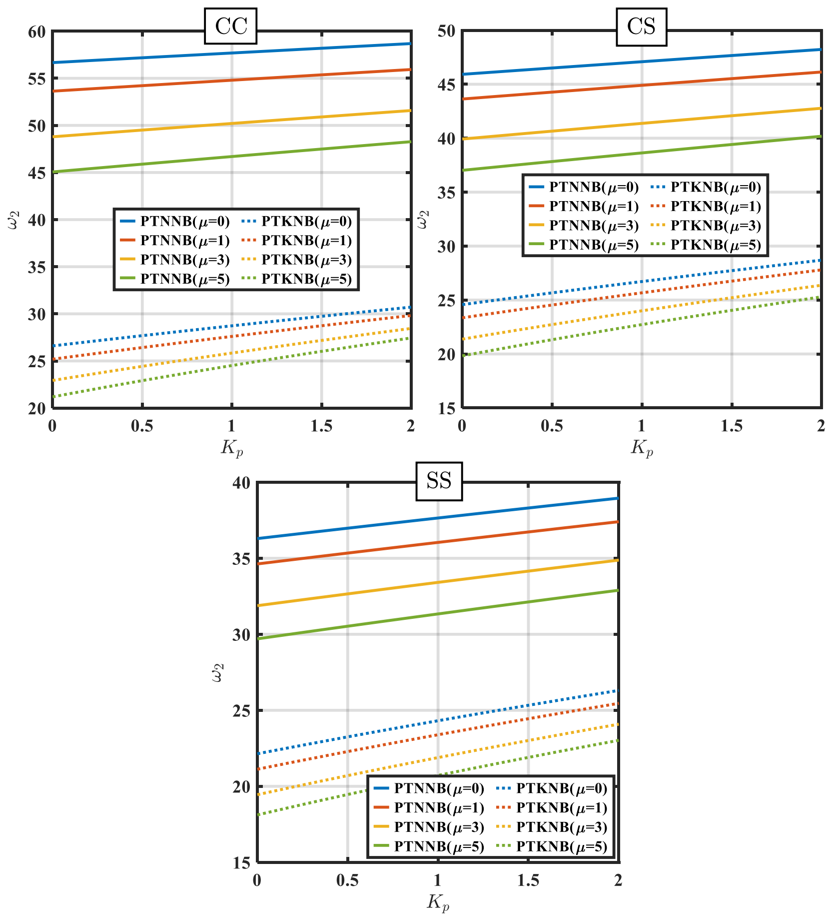

Fig. 6 Variation of the natural frequency parameter of the 2nd mode with Pasternak foundation parameter k_p for both PTNNB and PTKNB for SS, CC and CS boundary conditions at $N_0 = 4$, α=0.2, μ=0,1, 3,5 and L/h=15

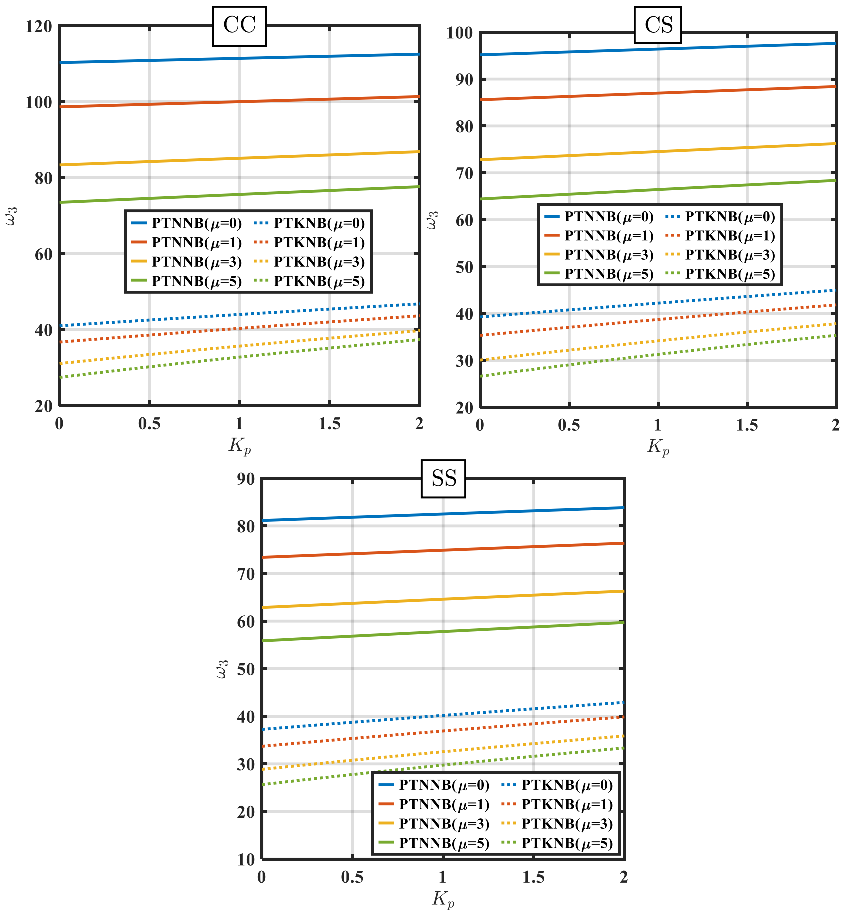

Fig. 7 Variation of the natural frequency parameter of the 3rd mode with Pasternak foundation parameter k_p for both PTNNB and PTKNB for SS, CC and CS boundary conditions at $N_0 = 4$, α=0.2, μ=0,1, 3,5 and L/h=15

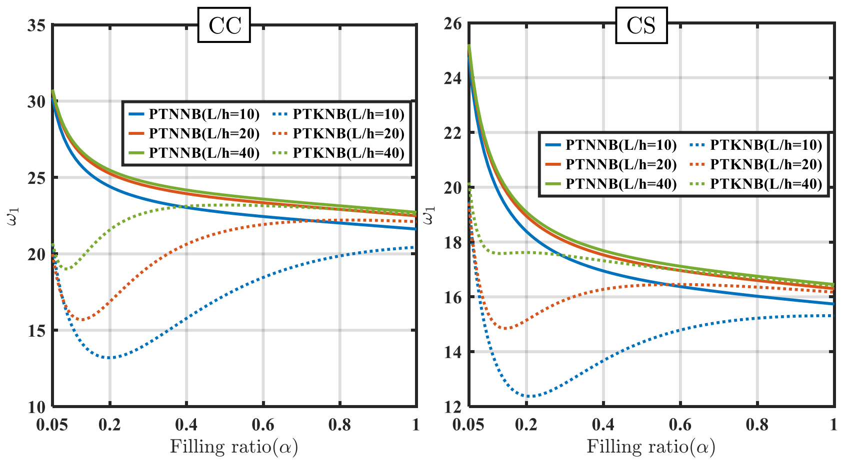

Fig. 8 Variation of the natural frequency of the 1st mode with the filling ratio for both PTNNB and PTKNB for SS, CC and CS boundary conditions at $N_0 = 2, \mu = 1, k_w = 20, k_p = 2$ and $L/h = 10, 20, 40$

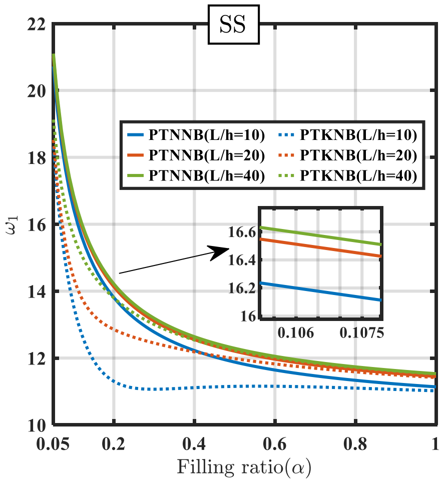

Fig. 8 Continued

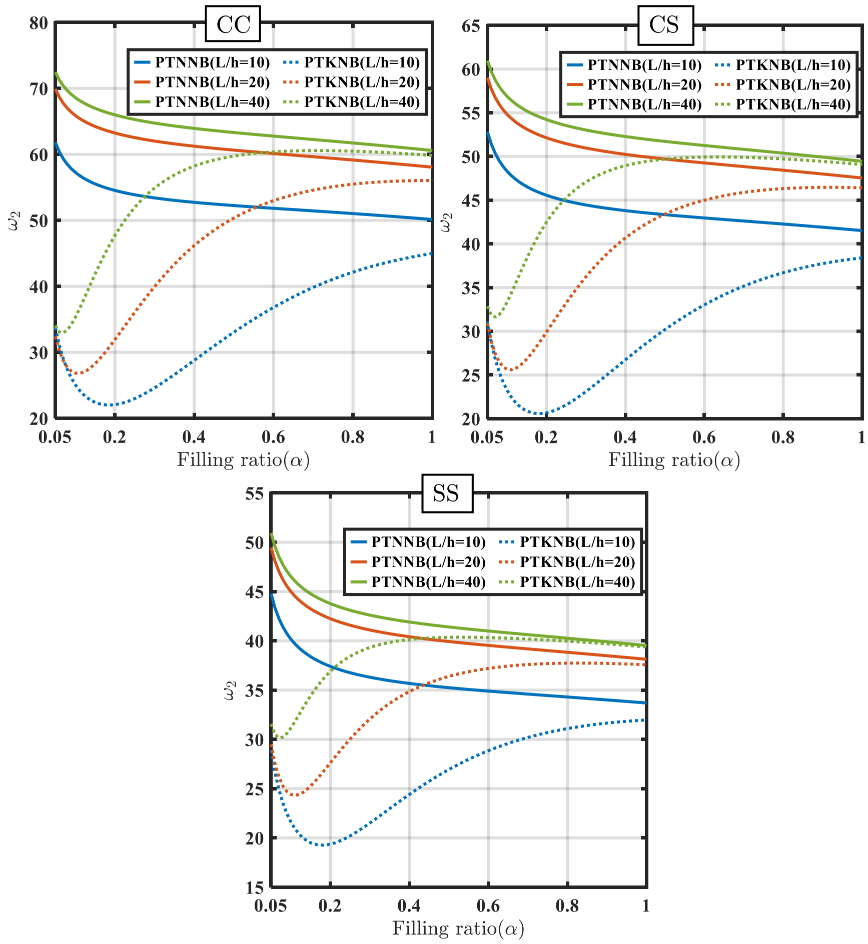

Fig. 9 Variation of the natural frequency of the 2nd mode with the filling ratio for both PTNNB and PTKNB for SS, CC and CS boundary conditions at $N_0 = 2, \mu = 1, k_w = 20, k_p = 2$ and $L/h = 10, 20, 40$

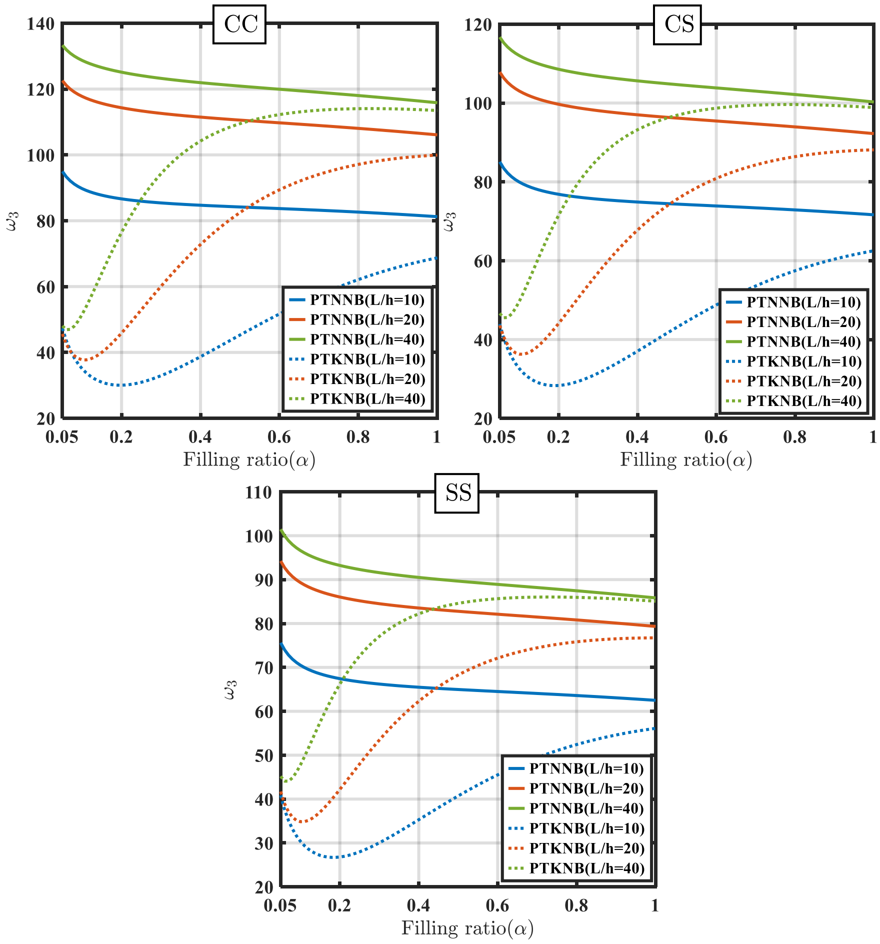

Fig. 10 Variation of the natural frequency of the 3rd mode with the filling ratio for both PTNNB and PTKNB for SS, CC and CS boundary conditions at $N_0 = 2, \mu = 1, k_w = 20, k_p = 2$ and $L/h = 10, 20, 40$

PTNNB. However, for PTKNB by increasing the filling ration, the natural frequency is decreased at first then increased. The modes of the natural frequency as the filling ratio approaching 1 and by increasing the beam aspect ratio, *L/h* the natural frequency almost becomes the same value for both cases PTNNB and PTKNB.

5.2.4 Effect of number of hole rows on PTNNB and PTKNB

The effect of the number of hole rows on the 1st, 2nd, and 3rd natural frequency modes is shown in Figs. 11-13 for perforated thin and thick nanobeams, respectively. As shown, by increasing the number of hole rows, the natural frequency decreases significantly in nonlinear behavior for PTNNB and PTKNB for all modes and boundary conditions, due to the reduction of the overall system stiffness. It is observed that, by increasing the beam aspect ratio the natural frequency modes are decreased. Also, the natural frequency overestimates at PTNNB than PTKNB for all modes and all boundary conditions even with an increase of the beam aspect ratio L/h.

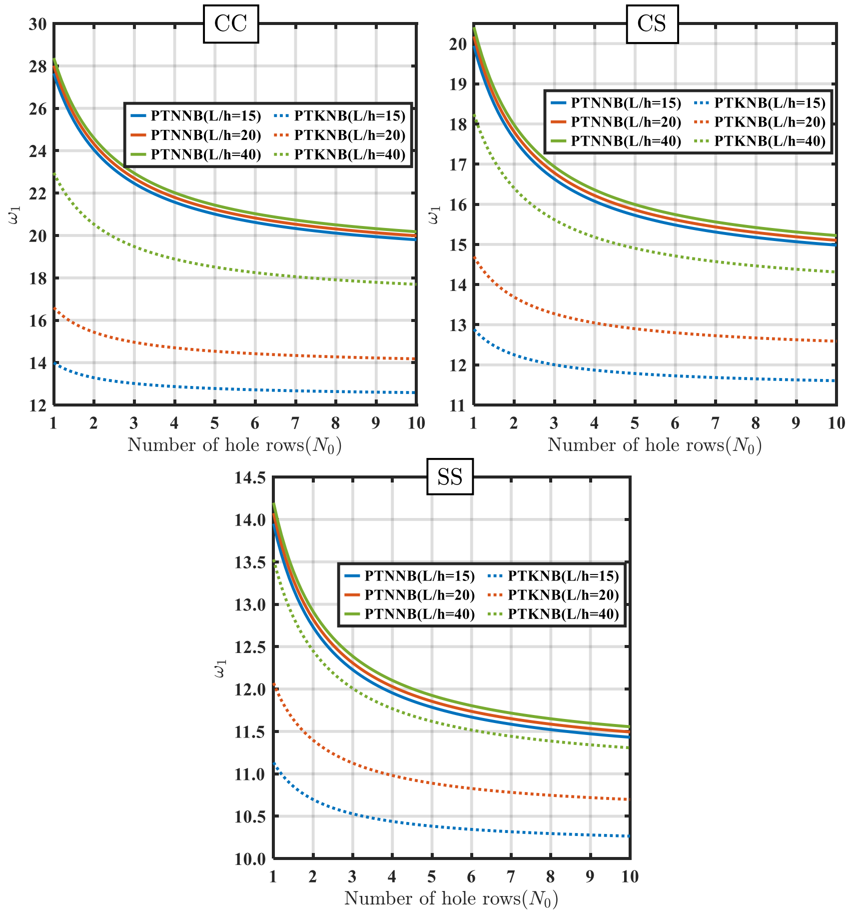

Fig. 11 Variation of the natural frequency of the 1st mode with the number of hole rows for both PTNNB and PTKNB for SS, CC and CS boundary conditions at $\alpha = 0.2, \mu = 1, k_w = 20, k_p = 2$ and $L/h = 15, 20, 40$

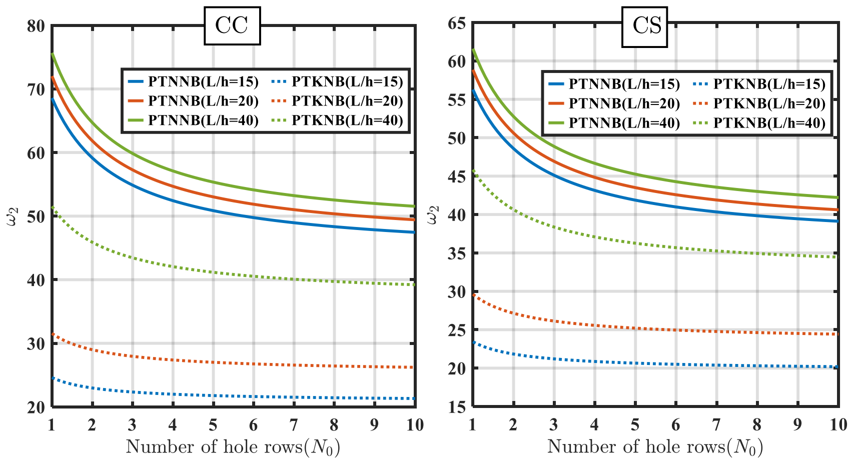

Fig. 12 Variation of the natural frequency of the 2nd mode with the number of hole rows for both PTNNB and PTKNB for SS, CC and CS boundary conditions at $\alpha = 0.2, \mu = 1, k_w = 20, k_p = 2$ and $L/h = 15, 20, 40$

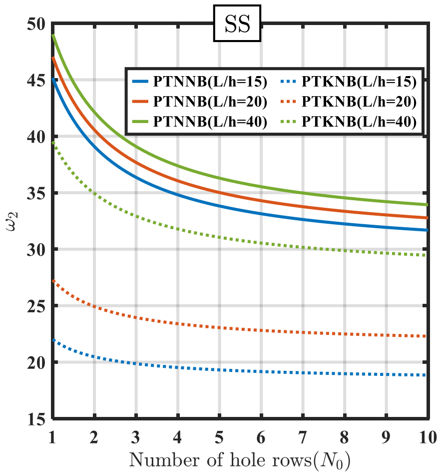

Fig. 12 Continued

5. Conclusions

The model developed in this article can be easily used in the analysis and design of perforated viscoelastic materials Nanobeam MEMS/NEMS Structures. The model investigates the dynamic response to vibrations of perforated viscoelastic material Nanostructure of thin/thick nanobeams with a size-dependent continuum pattern under different boundaries Conditions. The perforation is assumed to be arranged in a symmetrical array with equal spacing and hole geometry. The nanoscale size is incorporated into the model using the differential form of the non-local Eringen model. That The Kelvin viscoelastic constitutive relationship is used to account for viscoelasticity and energy dissipationthe nanostructure. Closed-form solutions are derived in detail to simplify the engineering analysis process and designers. Based on the current results, this is the conclusion

√ The Winkler foundation has great influence on the natural frequency of thin and thick perforated.

√ Nanobeam for all boundary conditions, by increasing Winkler foundation, the natural frequency increased significantly in nonlinear behavior for PTNNB. However, the Winkler foundation has insignificant effect in the case of PTkNB.

√ The effect of number of hole rows on the 1st, 2st, 3st natural frequency of perforated thin and thick nanobeams at 1st mode, 2nd mode, 3rd mode, respectively. by increasing the number of hole rows, the natural frequency decreases significantly in nonlinear behavior for PTNNB.

√ However, the number of hole rows has insignificant effect in case of PTKNB.

√ The Winkler foundation on the natural frequencies is increased for higher mode rather than lower ones for all boundary conditions.

√ The filling ratio on the 1st natural frequency of perforated thin and thick nanobeams. for CC, CS boundary condition by increasing filling ratio, the natural frequency decreases in case of PTNNB.

√ However, in case of PTKNB the filling ratio deceases until 0.1 then incrase for SS boundary condition by increasing filling ratio, the natural frequency decreases in case of PTNNB, PTKNB

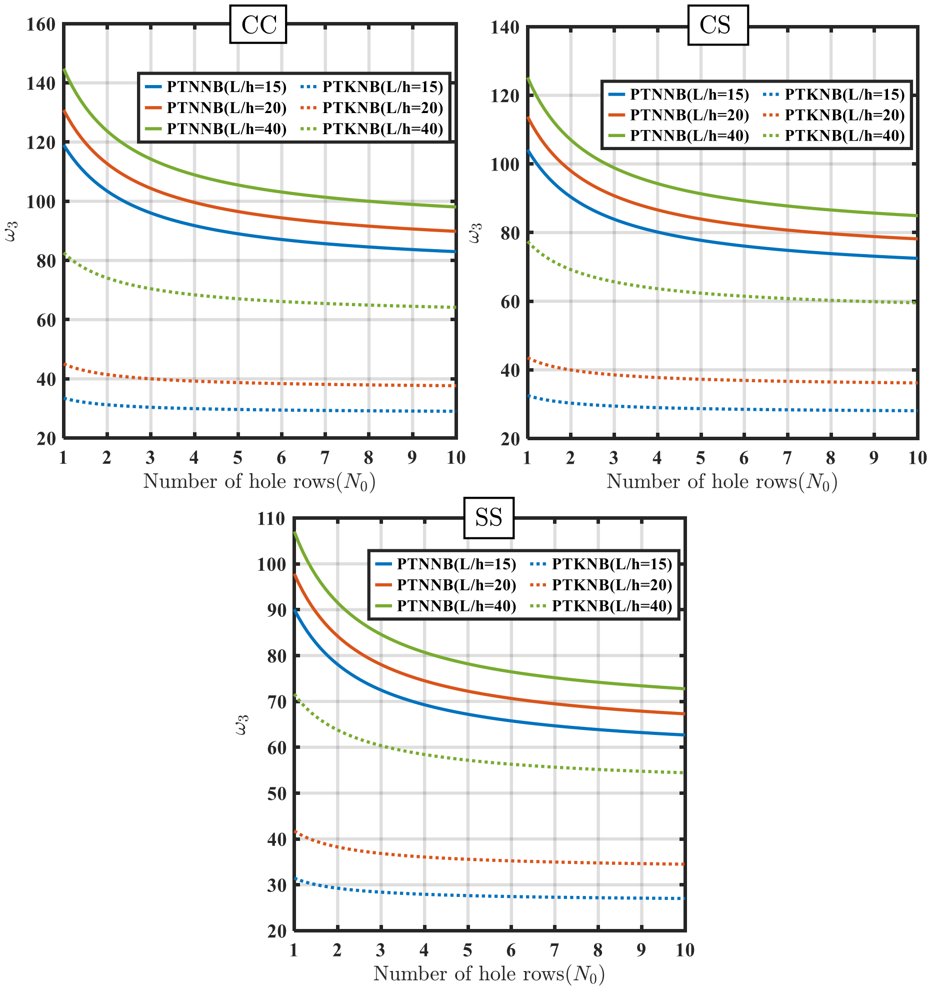

Fig. 13 Variation of the natural frequency of the 3rd mode with the number of hole rows for both PTNNB and PTKNB for SS, CC and CS boundary conditions at $\alpha = 0.2, \mu = 1, k_w = 20, k_p = 2$ and $L/h = 15, 20, 40$

References

Abdelrahman, A.A., Shanab, R.A., Esen, I. and Eltaher, M.A. (2022), "Effect of moving load on dynamics of nanoscale Timoshenko CNTs embedded in elastic media based on doublet mechanics theory", *Steel Compos. Struct.*, **44**(2), 241-256. https://doi.org/10.12989/scs.2022.44.2.241.

Abo-bakr, R.M., Shanab, R.A. and Attia, M.A. (2021), "Multi-objective optimization for lightweight design of bi-directional functionally graded beams for maximum frequency and buckling load", *Compos. Struct.*, **278**, 114691. https://doi.org/10.1016/j.compstruct.2021.114691.

Abouelregal, A.E. and Sedighi, H.M. (2022), "Thermoelastic characteristics of moving viscoelastic nanobeams based on the nonlocal couple stress theory and dual-phase lag model", *Physica Scripta*, **97**(11), 114003. https://doi.org/10.1088/1402-4896/ac97cc.

Abouelregal, A.E., Mohammad-Sedighi, H., Shirazi, A.H., Malikan, M. and Eremeyev, V.A. (2022), "Computational analysis of an infinite magneto-thermoelastic solid periodically dispersed with varying heat flow based on non-local Moore–Gibson–Thompson approach", *Continuum. Mech. Thermodyn.*, **34**(4), 1067-1085. https://doi.org/10.1007/s00161-021-00998-1.

Abouelregal, A.E., Nasr, M.E., Moaaz, O. and Sedighi, H.M. (2023), "Thermo-magnetic interaction in a viscoelastic micropolar medium by considering a higher-order two-phase-delay thermoelastic model", *Acta Mechanica*, **234**(6), 2519-2541. https://doi.org/10.1007/s00707-023-03513-6.

Alasadi, A.A., Ahmed, R.A. and Faleh, N.M. (2019), "Analyzing nonlinear vibrations of metal foam nanobeams with symmetric and non-symmetric porosities", *Adv. Aircraft Spacecraft Sci.*, **6**(4), 273-282. https://doi.org/10.12989/aas.2019.6.4.273.

Alazwari, M.A., Daikh, A.A. and Eltaher, M.A. (2022b), "Novel quasi 3D theory for mechanical responses of FG-CNTs reinforced composite nanoplates", *Adv. Nano Res.*, **12**(2), 117-137. https://doi.org/10.12989/anr.2022.12.2.117.

Alazwari, M.A., Esen, I., Abdelrahman, A.A., Abdraboh, A.M. and Eltaher, M.A. (2022a), "Dynamic analysis of functionally graded (FG) nonlocal strain gradient nanobeams under thermo-magnetic fields and moving load", *Adv. Nano Res.*, **12**(3), 231-251. https://doi.org/10.12989/anr.2022.12.3.231.

Ali, I.A., Alazwari, M.A., Eltaher, M.A. and Abdelrahman, A.A. (2022), "Effects of viscoelastic bonding layer on performance of piezoelectric actuator attached to elastic structure", *Mater. Res. Expr.*, **9**(4), 045701. https://doi.org/10.1088/2053-1591/ac5cae.

Alzahrani, E.O., Zenkour, A.M. and Sobhy, M. (2013), "Small scale effect on hygro-thermo-mechanical bending of nanoplates embedded in an elastic medium", *Compos. Struct.*, **105**, 163-172. http://doi.org/10.1016/j.compstruct.2013.04.045.

Ansari, R., Oskouie, M.F. andGholami, R. (2016), "Size-dependent geometrically nonlinear free vibration analysis of fractional viscoelastic nanobeams based on the nonlocal elasticity theory", *Physica E*, **75**, 266-271. http://doi.org/10.1016/j.physe.2015.09.022.

Ansari, R., Oskouie, M.F., Sadeghi, F. and Bazdid-Vahdati, M. (2015), "Free vibration of fractional viscoelastic Timoshenko nanobeams using the nonlocal elasticity theory", *Physica E*, **74**, 318-327. http://doi.org/10.1016/j.physe.2015.07.013.

Assie, A.E., Eltaher, M.A. and Mahmoud, F.F. (2010a), "The response of viscoelastic-frictionless bodies under normal impact", *Int. J. Mech. Sci.*, **52**(3), 446-454. https://doi.org/10.1016/j.ijmecsci.2009.11.005.

Assie, A.E., Eltaher, M.A. and Mahmoud, F.F. (2010b), "Modeling of viscoelastic contact-impact problems", *Appl. Math. Model.*, **34**(9), 2336-2352. https://doi.org/10.1016/j.apm.2009.11.001.

Assie, A.E., Mohamed, S.M., Shanab, R.A., Abo-bakr, R.M. and Eltaher, M.A. (2023), "Static buckling of 2D FG porous plates resting on elastic foundation based on unified shear theories", *J. Appl. Comput. Mech.*, **9**(1), 239-258. https://doi.org/10.22055/jacm.2022.41265.3723.

Bagheri, R. and Tadi Beni, Y. (2021), "On the size-dependent nonlinear dynamics of viscoelastic/flexoelectric nanobeams", *J. Vib. Control*, **27**(17-18), 2018-2033. https://doi.org/10.1177/1077546320952225.

Behdad, S., Fakher, M. and Hosseini-Hashemi, S. (2021), "Dynamic stability and vibration of two-phase local/nonlocal VFGP nanobeams incorporating surface effects and different boundary conditions", *Mech. Mater.*, **153**, 103633. https://doi.org/10.1016/j.mechmat.2020.103633.

Daikh, A.A., Houari, M.S.A. and Eltaher, M.A. (2021), "A novel nonlocal strain gradient Quasi-3D bending analysis of sigmoid functionally graded sandwich nanoplates", *Compos. Struct.*, **262**, 113347. https://doi.org/10.1016/j.compstruct.2020.113347.

Darban, H., Luciano, R., Caporale, A. and Basista, M. (2022), "Modeling of buckling of nanobeams embedded in elastic medium by local-nonlocal stress-driven gradient elasticity theory", *Compos. Struct.*, **297**, 115907. https://doi.org/10.1016/j.compstruct.2022.115907.

Demir, C., Mercan, K., Numanoglu, H.M. and Civalek, O. (2018), "Bending response of nanobeams resting on elastic foundation", *J. Appl. Comput. Mech.*, **4**(2), 105-114. https://doi.org/10.22055/JACM.2017.22594.1137.

Ding, H.X., Eltaher, M.A. and She, G.L. (2023), "Nonlinear low-velocity impact of graphene platelets reinforced metal foams cylindrical shell: Effect of spinning motion and initial geometric imperfections", *Aerosp. Sci. Technol.*, **140**, 108435. https://doi.org/10.1016/j.ast.2023.108435.

Ebrahimi, F. and Fardshad, R.E. (2018), "Dynamic modeling of nonlocal compositionally graded temperature-dependent beams", *Adv. Aircraft Spacecraft Sci.*, **5**(1), 141. https://doi.org/10.12989/aas.2018.5.1.141.

Ebrahimi, F. and Heidari, E. (2018), "Surface effects on nonlinear vibration and buckling analysis of embedded FG nanoplates via refined HOSDPT in hygrothermal environment considering physical neutral surface position", *Adv. Aircraft Spacecraft Sci.*, **5**(6), 691. https://doi.org/10.12989/aas.2018.5.6.691.

Ebrahimi, F., Babaei, R. and Shaghaghi, G.R. (2018), "Nonlocal buckling characteristics of heterogeneous plates subjected to various loadings", *Adv. Aircraft Spacecraft Sci.*, **5**(5), 515. https://doi.org/10.12989/aas.2018.5.5.515.

Ebrahimi, F., karimiasl, M. and Mahesh, V. (2021), "Chaotic dynamics and forced harmonic vibration analysis of magneto-electro-viscoelastic multiscale composite nanobeam", *Eng. Comput.*, **37**(2), 937-950. https://doi.org/10.1007/s00366-019-00865-3.

Eltaher, M.A. and Mohamed, N. (2020a), "Nonlinear stability and vibration of imperfect CNTs by doublet mechanics", *Appl. Math. Comput.*, **382**, 125311. https://doi.org/10.1016/j.amc.2020.125311.

Eltaher, M.A., Agwa, M. and Kabeel, A. (2018), "Vibration analysis of material size-dependent CNTs using energy equivalent model", *J. Appl. Comput. Mech.*, **4**(2), 75-86. https://doi.org/10.22055/JACM.2017.22579.1136.

Eltaher, M.A., Mohamed, N. and Mohamed, S.A. (2020b), "Nonlinear buckling and free vibration of curved CNTs by doublet mechanics", *Smart Struct. Syst.*, **26**(2), 213-226. https://doi.org/10.12989/sss.2020.26.2.213.

Eltaher, M.A., Shanab, R.A. and Mohamed, N.A. (2022), "Analytical solution of free vibration of viscoelastic perforated nanobeam", *Arch. Appl. Mech.*, **93**(1), 221-243. https://doi.org/10.1007/s00419-022-02184-4.

Eringen, A.C. (1972), "Nonlocal polar elastic continua", *Int. J. Eng. Sci.*, **10**(1), 1-16. https://doi.org/10.1016/0020-7225(72)90070-5.

Eringen, A.C. (1983), "On differential equations of nonlocal elasticity and solutions of screw dislocation and surface waves", *J. Appl. Phys.*, **54**(9), 4703-4710. https://doi.org/10.1063/1.332803.

Fenjan, R.M., Hamad, L.B. and Faleh, N.M. (2020), "Mechanical-hygro-thermal vibrations of functionally graded porous plates with nonlocal and strain gradient effects", *Adv. Aircraft Spacecraft Sci.*, **7**(2), 169-186. https://doi.org/10.12989/aas.2020.7.2.169.

Hieu, D.V., Chan, D.Q. and Sedighi, H.M. (2021b), "Nonlinear bending, buckling and vibration of functionally graded nonlocal strain gradient nanobeams resting on an elastic foundation", *J. Mech. Mater. Struct.*, **16**(3), 327-346. https://doi.org/10.2140/jomms.2021.16.327.

Hieu, D.V., Hoa, N.T., Duy, L.Q. and Kim Thoa, N.T. (2021a), "Nonlinear vibration of an electrostatically actuated functionally graded microbeam under longitudinal magnetic field", *J. Appl. Comput. Mech.*, **7**(3), 1537-1549. https://doi.org/10.22055/JACM.2021.35504.2670.

Hossain, M.M. and Lellep, J. (2021), "Mode shape analysis of dynamic behaviour of cracked nanobeam on elastic foundation", *Eng. Res. Expr.*, **3**(4), 045003. https://doi.org/10.1088/2631-8695/ac2a75.

Hosseini, S.A.H., Moghaddam, M.H. and Rahmani, O. (2020), "Exact solution for axial vibration of the power, exponential and sigmoid FG nonlocal nanobeam", *Adv. Aircraft Spacecraft Sci.*, **7**(6), 517-536. https://doi.org/10.12989/aas.2020.7.6.517.

Jalaei, M.H., Thai, H.T. and Civalek, Ö. (2022), "On viscoelastic transient response of magnetically imperfect functionally graded nanobeams", *Int. J. Eng. Sci.*, **172**, 103629. https://doi.org/10.1016/j.ijengsci.2022.103629.

Khadir, A.I., Daikh, A.A. and Eltaher, M.A. (2021), "Novel four-unknowns quasi 3D theory for bending, buckling and free vibration of functionally graded carbon nanotubes reinforced composite laminated nanoplates", *Adv. Nano Res.*, **11**(6), 621-640. https://doi.org/10.12989/anr.2021.11.6.621.

Khorshidi, M.A. (2021), "Postbuckling of viscoelastic micro/nanobeams embedded in visco-Pasternak foundations based on the modified couple stress theory", *Mech. Time-Depend. Mater.*, **25**(2), 265-278. https://doi.org/10.1007/s11043-019-09439-8.

Malikan, M. and Far, M.N. (2018), "Differential quadrature method for dynamic buckling of graphene sheet coupled by a viscoelastic medium using neperian frequency based on nonlocal elasticity theory”, *J. Appl. Comput. Mech.*, **4**(3), 147-160. https://doi.org/10.22055/JACM.2017.22661.1138.

Malikan, M., Nguyen, V.B. and Tornabene, F. (2018), “Damped forced vibration analysis of single-walled carbon nanotubes resting on viscoelastic foundation in thermal environment using nonlocal strain gradient theory”, *Eng. Sci. Technol.*, **21**(4), 778-786. https://doi.org/10.1016/j.jestch.2018.06.001.

Martin, O. (2022), “Nonlinear vibrations of fractional nonlocal viscoelastic nanotube resting on a Kelvin–Voigt foundation”, *Mech. Adv. Mater. Struct.*, **29**(19), 2769-2779. https://doi.org/10.1080/15376494.2021.1878401.

Mechab, B., Mechab, I., Benaissa, S., Ameri, M. and Serier, B. (2016), “Probabilistic analysis of effect of the porosities in functionally graded material nanoplate resting on Winkler–Pasternak elastic foundations”, *Appl. Math. Model.*, **40**(2), 738-749. http://dx.doi.org/10.1016/j.apm.2015.09.093.

Mindlin, R.D. (1962), *Influence of Couple-Stresses on Stress Concentrations*, Columbia University at New York.

Mindlin, R.D. (1965), “Second gradient of strain and surface-tension in linear elasticity”, *Int. J. Solid. Struct.*, **1**(4), 417-438. https://doi.org/10.1016/0020-7683(65)90006-5.

Mohamed, N., Eltaher, M.A., Mohamed, S.A. and Seddek, L.F. (2018), “Numerical analysis of nonlinear free and forced vibrations of buckled curved beams resting on nonlinear elastic foundations”, *Int. J. Nonlin. Mech.*, **101**, 157-173. https://doi.org/10.1016/j.ijnonlinmec.2018.02.014.

Mohamed, N., Eltaher, M.A., Mohamed, S.A. and Seddek, L.F. (2019), “Energy equivalent model in analysis of postbuckling of imperfect carbon nanotubes resting on nonlinear elastic foundation”, *Struct. Eng. Mech.*, **70**(6), 737-750. https://doi.org/10.12989/sem.2019.70.6.737.

Mohammadi, H., Mahzoon, M., Mohammadi, M. and Mohammadi, M. (2014), “Postbuckling instability of nonlinear nanobeam with geometric imperfection embedded in elastic foundation”, *Nonlin. Dyn.*, **76**(4), 2005-2016. https://doi.org/10.1007/s11071-014-1264-x.

Nadeem, M., He, J.H., He, C.H., Sedighi, H.M. and Shirazi, A. (2022). “A numerical solution of nonlinear fractional newell-whitehead-segel equation using natural transform”, *Twms J. Pure Appl. Math.*, **13**(2), 168-182.

Nix, W.D. and Gao, H. (1998), “Indentation size effects in crystalline materials: a law for strain gradient plasticity”, *J. Mech. Phys. Solid.*, **46**(3), 411-425. https://doi.org/10.1016/S0022-5096(97)00086-0.

Noroozi, M. and Ghadiri, M. (2021), “Nonlinear vibration and stability analysis of a size-dependent viscoelastic cantilever nanobeam with axial excitation”, *Proc. Inst. Mech. Eng., Part C: J. Mech. Eng. Sci.*, **235**(18), 3624-3640. https://doi.org/10.1177/0954406220959104.

Rahmani, A., Faroughi, S., Sari, M. and Abdelkefi, A. (2022), “Selection of size dependency theory effects on the wave’s dispersions of magneto-electro-thermo-elastic nano-beam resting on visco-elastic foundation”, *Eur. J. Mech.-A/Solid.*, **95**, 104620. https://doi.org/10.1016/j.euromechsol.2022.104620.

Ramezannejad Azarboni, H. and Heidari, H. (2022), “Nonlinear primary frequency response analysis of self-sustaining nanobeam considering surface elasticity”, *J. Appl. Comput. Mech.*, **8**(4), 1196-1207. https://doi.org/10.22055/JACM.2020.33977.2317.

Reza, A., Shishesaz, M. and Sedighi, H.M. (2021), “Micromechanical approach to viscoelastic stress analysis of a pin-loaded hole in unidirectional laminated PMC”, *Polym. Polymer Compos.*, **29**(9), S1144-S1157. https://doi.org/10.1177/09673911211047340.

Togun, N. (2016), “Nonlocal beam theory for nonlinear vibrations of a nanobeam resting on elastic foundation”, *Bound. Value Prob.*, **6**(1), 1-14. https://doi.org/10.1186/s13661-016-0561-3.

Togun, N. and Bağdatlı, S.M. (2016), “Nonlinear vibration of a nanobeam on a Pasternak elastic foundation based on non-local Euler-Bernoulli beam theory”, *Math. Comput. Appl.*, **21**(1), 3. https://doi.org/10.3390/mca21010003.

Toupin, R. (1962), “Elastic materials with couple-stresses”, *Arch. Ration. Mech. Anal.*, **11**(1), 385-414.

Wu, Q., Yao, M. and Niu, Y. (2022), “Nonplanar free and forced vibrations of an imperfect nanobeam employing nonlocal strain gradient theory”, *Commun. Nonlin. Sci. Numer. Simul.*, **114**, 106692. https://doi.org/10.1016/j.cnsns.2022.106692.

You, H., Lim, H.J. and Yun, G.J. (2022). “A micromechanics-based time-domain viscoelastic constitutive

model for particulate composites: Theory and experimental validation", *Adv. Aircraft Spacecraft Sci.*, **9**(3), 217-242. https://doi.org/10.12989/aas.2022.9.3.217.
Zenkour, A.M. (2017), "Vibration analysis of generalized thermoelastic microbeams resting on Visco-Pasternak", *Adv. Aircraft Spacecraft Sci.*, **4**(3), 267. https://doi.org/10.12989/aas.2017.4.3.267.
Zheng, Y.F., Qu, D.Y., Liu, L.C. and Chen, C.P. (2023), "Size-dependent nonlinear bending analysis of nonlocal magneto-electro-elastic laminated nanobeams resting on elastic foundation", *Int. J. Nonlin. Mech.*, **148**, 104255. https://doi.org/10.1016/j.ijnonlinmec.2022.104255.

CC